SLAC TRANS 36

Sistema kratnogo uskoreniya elektrodinamicheskogo separatora chastits vysokikh energiĭ, (Multiple acceleration system for an electrodynamic separator of high-energy particles), by N.G. Borisov et al. Joint Institute of Nuclear Research, Dubna, 1965. JINR-P-2375, 13 pp. Translated from the Russian (January 1966) by T. Watt.

TRANSLATED FOR
STANFORD LINEAR ACCELERATOR CENTER

****
****
****

MULTIPLE ACCELERATION SYSTEM FOR AN ELECTRODYNAMIC SEPARATOR OF HIGH-ENERGY PARTICLES

by

N.G.Borisov, V.A.Vagin, V.D.Volodin, V.I.Zaitsev, N.N.Plyashkevich, A.P. Saeynko, I.N.Semenyushkin and V. L. Stepanyuk.

Introduction

The electromagnetic separator of high-energy particles at the Joint Institute of Nuclear Research, which is based on the principle of high-frequency separation of particles according to their masses, incorporates a system of multiple acceleration of protons at the frequency f_p = 149, 550 Mc/s. This principle was put forward in 1957 by Veksler and Petukhov[1,4].

The multiple acceleration system ensures the capture of protons accelerated to maximum energy into the acceleration process at a multiple frequency (multiplicity factor $q = 104$) and the particles continue to be accelerated at this frequency for 15-20 μsec. A periodic train of short bunches of secondary particles, which are necessary for the separation of the beam by the high-frequency deflector, is formed during the subsequent interaction of the captured beam with the target.

2. Block diagram and chief parameters of the apparatus

One of the chief parameters of the multiple acceleration system (and of the electrodynamic separator as a whole) is the working frequency f_p. From the point of view of the overall length of the separator and of the dimensions of the high-frequency devices, the frequency f_p should be as high as possible. On the other hand, an increase in f_p, and consequently, in the multiplicity factor q, is associated with an increase in the resonator slit voltage U_p which is necessary to achieve the required capture factor. Moreover, the

maximum value of f_p is restricted by the aperture of the proton synchrotron chamber (2000 x 500 mm^2). The working wavelength λ_p must be greater than the critical value for the fundamental mode E_{11} excited by the resonators in the chamber. The critical wavelength for the E_{11} mode is $\lambda_{cr\ 1} = 1$ m. However, owing to the very slight geometric asymmetry in the construction of the resonator, the lowest H_{01} mode can be excited in the chamber as a result of manufacturing faults, deformation during the running of the machine, etc. The critical wavelength for this mode is $\lambda_{cr\ 2} = 4$ m. It follows that, to prevent the entry of high-frequency power into the chamber, we must ensure that $\lambda_p > \lambda_{cr\ 2}$. The working wavelength was therefore chosen to be $\lambda_p = 2$ m. The decisive factor turned out to be the total length of the separator. It is important to note, however, that the condition $\lambda_p < \lambda_{cr\ 2}$ gave rise to additional difficulties connected with the necessity of suppressing radiation in the H_{01} mode.

In order to obtain a high enough proton capture factor ($\sigma \simeq 0.7$) for the multiple acceleration process at the chosen working frequency, the resultant amplitude of the accelerating voltage in the resonators

must be $U_p \simeq 250$ kv. This amplitude was determined from curve 1 in Figure 2, which in turn was calculated[1-3] for a 10 Gev proton beam with an energy spread of $\pm$ 2.8 Mev and a multiplicity $q = 104$. It is evident from this curve that an appreciable increase in σ with increasing U_p occurs only up to values of σ in the range 0.65 - 0.75.

The proton-capture efficiency depends also on the precision with which the variable accelerating frequency of the proton synchrotron $f_{1(t)}$ at the beginning of the multiple acceleration process corresponds to the multiple value f_{1q}, i.e. the accuracy with which the condition

$$f_{1q} = \frac{f_p}{q}. \qquad (1)$$

is satisfied. For the maximum amplitude of radial-phase oscillations of protons at the end of the acceleration cycle $\rho_A = \pm$ 2.1 cm (ref. 2), which corresponds to a frequency deviation $\Delta f_{1\rho} = \pm$ 900 c/s, the maximum permissible error in f_{1q} at the instant when the multiple acceleration system is switched on must be

$$\Delta f_{1q} \leq \pm 0{,}1\, \Delta f_{1\rho} \simeq \pm 100 \text{ c/s}. \qquad (2)$$

A block diagram of the multiple acceleration system is shown in Figure 1. The system is operated with the aid of the frequency comparison circuit 1. The blanking circuit 2 prevents further operation of the system while the magnetic field of the accelerator is falling. The pulse modulator is used to shape the high-voltage pulses reaching the anodes of the generator tubes. The two final stages of the high-frequency generators 11, 12 supply the resonators 16, 17 independently through rigid coaxial feeders. Phasing of the resonator voltage is achieved by the phase-shifter 13, which is capable of varying the phase continuously between 0 and 180^{o}. Reflectometers 14, 15 are used to control the matching and the power level fed into the resonator.

3. Description of the apparatus

Each of the two resonators takes the form of a quarter-wave section of a coaxial line with a rectangular transverse cross-section. The areas of the external and internal conductors are 495 x 1750 and 310 x 1565 mm^2 respectively. The total length of the resonator

without the screens is 505 mm. With the screens (used for shielding purposes), the length is 1360 mm. The intrinsic Q-factor is Q_o = 5000, the shunt resistance is R_{sh} = 40 kohm, and the power fed into each resonator is P = 150 kw. Resonance high-frequency discharge is prevented by a set of electrodes, suitably arranged inside the resonator and maintained at -2 kv. The resonator H_{01} mode, which is excited as a result of slight asymmetry in the system, is suppressed by adjusting the resonator after insertion into the chamber.

The high-frequency generators (Figure 3) consist of five power generators with independent excitation in coaxial line sections. The first generator is based on the GU-37B tube and the remaining four on GI-24A. A schematic diagram of one of the generators based on GI-24A is shown in Figure 4. The anode line of generator 5 has a length of $3\lambda/4$. The anode blocking capacitance 3 is located on the internal conductor of the line at a current node. The anode circuit is tuned by means of the shorting plunger 6 which is operated by remote control through the lead 7. The cathode circuit is tuned with the aid of the

capacitive stub 10. A power of P_{in} = 500 w is fed into the input of the generators. It is derived from a three-stage preamplifier (Figure 5) which is located in a separate stand (Figure 3). The preamplifier incorporates the 6N3P (L 1), GU-32 (L2), and GU-29 (L3) tubes. The circuits of the last two stages (L_4, L_5, L_6, L_7) are made in the form of two-conductor lines. The circuits of the first stage (L_1, L_2, and L_3) consist of elements with lumped parameters. A power of P_{in} = 0.5 w is fed into the preamplifier from a quartz-stabilized master generator.

The pulse modulator (Figures 6 and 7) has the following parameters: power per pulse P_u = 1 Mw, pulse length r_u = 15-20 μsec, Q = 450, rise time $r_{\varphi 1}$ = 1.5 μsec, decay time $r_{\varphi 2}$ = 2 μsec, slope at maximum δ = 15%. The modulator is based on GI-18B tubes in a circuit involving partial discharge of capacitance. The circuit was selected so as to obtain maximum flexibility in the parameters of the output pulse from the modulator and lack of sensitivity to the load (generators) whose resistance may vary considerably during detuning or breakdown in the resonators. The characteristics of the GI-18B, GI-24A, GU-37B, and

GU-29 tubes, and the other devices employed, were designed for pulse lengths of less than 1000 μsec, but existing data[5,6] show that they can be used for lengths up to 50 μsec without substantial deterioration in the parameters. The last (L_2, L_3, and L_4) and the penultimate (L_1) modulator stages were in the form of cathode loaded pulse amplifiers in order to obtain positive polarities. The design of a pulse transformer capable of handling 1 Mw for pulse lengths of 15-20 μsec presented considerable difficulties, and they were therefore not used in the final stages of the modulator. The pulse transformer Tr.1 was used only at the input of L_1 where the power level is 1.5 kw. The main parameters of this transformer are as follows: Cross-section of iron core S = 72 cm^2, number of primary turns W_1 = 3500, number of secondary turns W_2 = 2000 ; the layers of the secondary lie between layers of the primary. Since the secondary of Tr.1 was at the full output voltage of the modulator, the parasitic capacitance between the transformer coils gave rise to feedback and hence to a deterioration in the rise times of the modulator pulse. To check this, the cathodes of the final tubes (L_2, L_3, and L_4)

were grounded (modulator with a negative polarity of the output pulse). The rise time of the modulator pulse was then only 0.1 μsec, which confirms the above assumption. The rectifiers (-200 v, + 6 kv and -600 v) and the secondaries of transformers Tr.1. Tr.2, Tr.3, Tr.4, and Tr.5 were at the full output modulator voltage. The capacitors C1, C2, and C3 consisted of type IM-3/100 elements.

The frequency comparison system 1 (Figure 1) consists of a quartz filter operating at 100 kc/s, a highly stabilized heterodyne with f_2 = 1535-1540 kc/s (stability 10^{-5}), and a mixer. The input of the mixer receives the variable frequency of the proton synchrotron, $f_{1(t)}$, and the heterodyne frequency f_r. The mixer produces the difference $f_r - f_{1(t)}$ which is fed into the quartz filter. The heterodyne frequency is set accurately at 100 c/s above f_{1q} = 1438 kc/s. The frequency comparison circuit then produces a pulse when the condition given by equation (1) is precisely satisfied. The accuracy of the system was found experimentally to be $\Delta f_{1q} = \pm$ 30 c/s. The frequency comparison-circuit triggers a four-channel fantastron delay system which is used to synchronize the remaining parts of the

separator. The fundamental accelerating frequency is suppressed with a delay of 2 μsec in order to prevent any change in the proton beam while the high-frequency voltage reaches a steady state. The operation of the entire system is controlled from a central control desk (Figure 8).

4. Experimental results

Experiments were carried out on the capture of accelerated protons into the multiple acceleration process with $q = 104$ at proton energy of 10 GeV. One resonator was employed with the slit voltage (amplitude) varied between 20 - 70 kv. The capture into the multiple acceleration process was recorded by inductive electrodes (for more details about the proton capture recording, see ref. 3). The experimental dependence of the proton-capture factor σ on the resonator slit voltage U_p is shown by curve 3 of Figure 2, which is not too different from the calculated result (curve 1). Curve 2 shows the results obtained in experiments involving a recently developed system for suppressing synchrotron oscillations. In this case, the energy spread of the accelerated beam was smaller than previously[2] ($\pm$ 1.7 Mev

instead of ± 2.8 Mev). It was therefore possible to obtain the required capture factor $\sigma \simeq 0.7$ with a resonator slit voltage $U_p = 70$ kv instead of the 250 kv required before.

Figure 9 shows the proton-capture factor σ as a function of the precision with which condition (1) was obeyed for a beam spread of ±1.7 Mev. It is evident from the figure that a departure of the frequency from the optimum value by 200 c/s gives rise to a reduction in σ from 0.60 to 0.50, i.e. by 20%. This confirms that the tolerance $\Delta f_q = \pm 100$ c/s, which we have chosen for the frequency comparison circuit, was satisfactory.

The phase characteristics of the system were investigated since the phase matching to the separator reflecting system should be $\Delta\varphi \lesssim \pm 10^\circ$. When the generator anode voltage is increased from 2.5 to 7 kv (corresponding to 70 kv on the resonator slit), the phase of the resonator slit voltage changes by 17° (at the beginning, this amounted to 7° per kv and, at 7 kv, the rate of change was 1.5° per kv). This phase change is due to a change in the generator cut-off angle and presents no particular difficulties since the system normally

operates at 7 kv. Moreover, a change in the phase was noted as the resonator warmed up during the operation. This change was of the order of 25° and occurred during the first two hours of operation. No changes in the phase were observed thereafter. Since the design of the resonator is such that water cooling with thermostated water cannot be employed, the necessary phase stability was achieved by a preliminary warm-up period of about two hours.

A study was made of the captured-beam energy spread due to the fact that the synchronization of the multiple acceleration system was achieved relative to the accelerating voltage of the proton synchrotron rather than relative to the magnetic field. The required energy spread in the captured beam ($\pm$ 0.5%) was observed only in 80% of all cases. In the remaining 20% of the cases it amounted to $\pm$ 1.5%. It was therefore subsequently assumed that, at the end of the acceleration cycle, the proton synchrotron goes over into an acceleration state at constant frequency f_{lq} = 1438.1 kc/s, and the synchronization of the multiple acceleration system was achieved relative to the magnetic field. This ensured an energy spread in

the captured beam of less than ± 0.3%.

The authors wish to express their gratitude to I.P. Golembevskaya, M.G. Golovoya, S.N. Plyashkevich and V.V. Shustrov for assistance during the setting up of the apparatus, and also to all Staff working on the proton synchrotron and to members of the electronics division of the HEL for assistance in the accelerator experiments.

References

1. V.N. Zubarev, V.S. Kladnitskiĭ, A.B. Kuznetsov, S.V. Mukhin, L.S. Okhrimenko, N.B. Rubin and I.N. Semenyushkin, JINR preprint P-371, Dubna 1959.

2. A.B. Kuznetsov and K.P. Myznikov, Atomnaya energiya 5, (1962) 373.

3. V.A. Vagin, A.D. Panfilov, I.N. Semenyushkin, V.L. Stepanyuk and K.V. Chekhlov, JINR Preprint 1406, Dubna 1963.

4. V.A. Vagin, V.I. Veksler, V.N. Zubarev, A.B. Kuznetsov, S.V. Mukhin, V.A. Petukhov, V.A. Popov, N.B. Rubin, I.N. Semenyushkin, V.L. Stepanyuk and K.V. Chekhlov, Trudy Mezhdunarodnoĭ konferentsii po uskoritelyam /Proceedings of the International Conference on Accelerators/, Dubna 1963.

5. V.A. Vagin, M. Vysochanskiĭ, S.V. Mukhin, S.V. Rikhvitskiĭ, I.N. Semenyushkin, V.L. Stepanyuk and I. Foltin, Trudy Mezhdunarodnoĭ konferentsii po uskoritelyam /Proceedings of the International Conference on Accelerators/, Dubna 1963.

6. V.A. Vagin, V.D. Volodin, A.D. Panfilov, N.N. Plyashkevich, A.P. Sayenko, I.N. Semenyushkin, V.L. Stepanyuk, K.V. Chekhlov and N.V. Shustrov, JINR Preprint 1478, Dubna 1963.

Received

September 28, 1965.

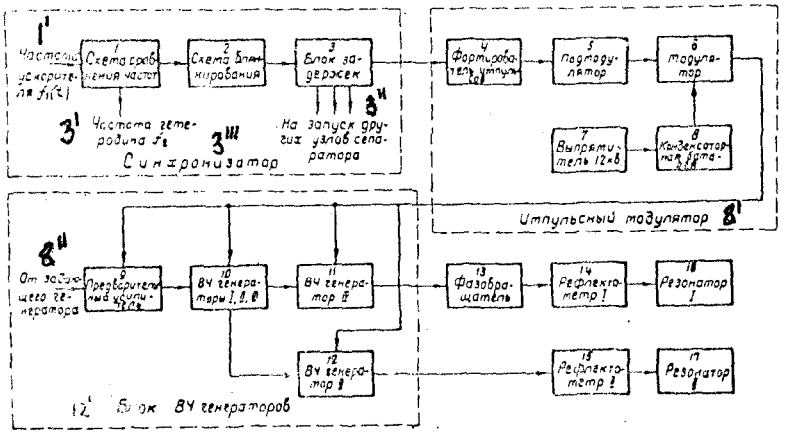

Рис. 1. Блок-схема установки.

F i g u r e 1: Block diagram of the apparatus

1' - accelerator frequency $f_{1(t)}$
1 - frequency comparison system
2 - blanking circuit
3 - delay block
3' - heterodyne frequency f_2
3" - triggering pulse for other parts of the separator
3"' - synchronizer
4 - pulse shaper
5 - premodulator
6 - modulator
7 - 12 kv rectifier
8 - capacitor bank
8' - pulse modulator
8" - from master generator
9 - preamplifier
10 - high-frequency generators I, II, III
11 - high-frequency generator IV
12 - high-frequency generator V
12' - HF generator block
13 - phase shifter
14 - reflectometer I
15 - reflectometer II
16 - resonator I
17 - resonator II

F i g u r e 2 :

Dependence of the proton-capture factor σ on the resonator slit voltage U_p. Proton energy 10 GeV, multiplicity q = 104, multiple acceleration frequency f_p = 149,550 Mc/s.

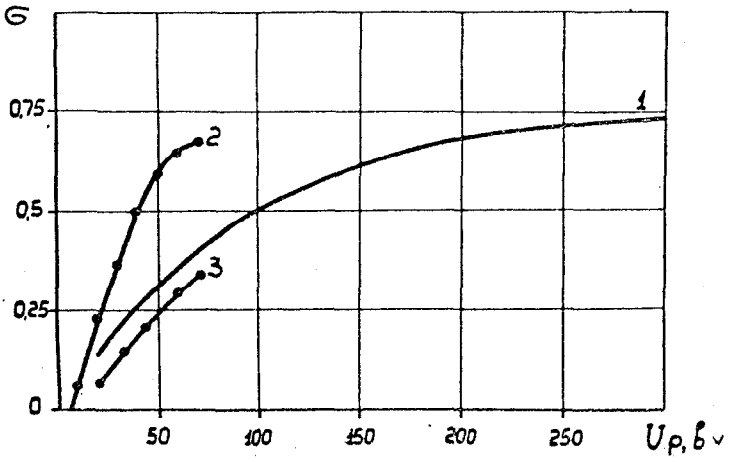

Рис. 2. Зависимость коэффициента перезахвата протонов в режим кратного ускорения σ от напряжения на щели резонаторов U_p. Энергия протонов E =10 Гэв, кратность q =104, частота кратного ускорения f_p =149,550 Мгц. 1 - расчетная кривая, энергетический спектр пучка $\Delta E = \pm 2{,}8$ Мэв; 2 - экспериментальная кривая - энергетический спектр пучка $\Delta E = \pm 1{,}7$ Мэв; 3 - экспериментальная кривая, энергетический спектр пучка $\Delta E = \pm 2{,}8$ Мэв.

1 - calculated with beam energy spread of $\pm$ 2.8 Mev

2 - experimental, with a beam spread of $\pm$ 1.7 Mev

3 - experimental, with a beam spread of $\pm$ 2.8 Mev

F i g u r e 3 :

Photograph of the high-frequency generators

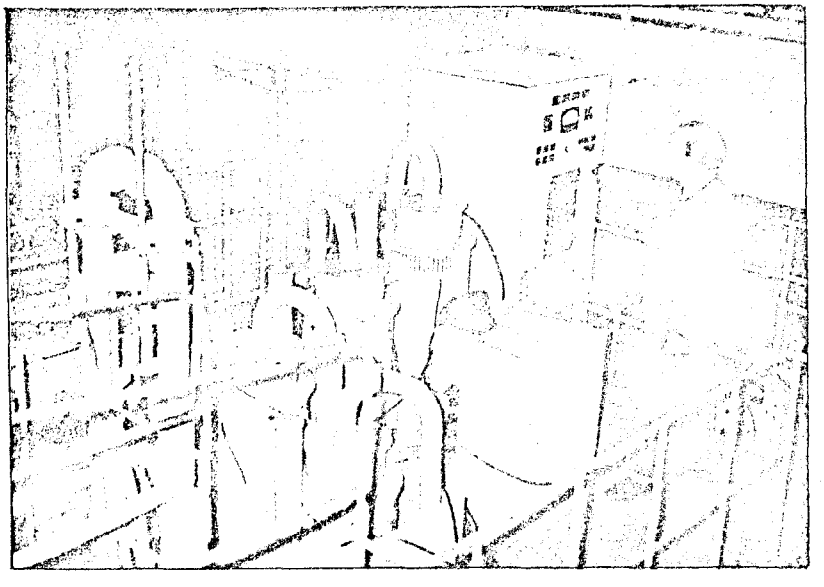

Рис. 3. Внешний вид блока высокочастотных генераторов.

F i g u r e 4 :

The GI-24A generator

1 - GI-24A tube
2 - water-cooling for the tube
3 - anode blocking capacitance
4 - insulator
5 - anode line
6 - plunger
7 - lead-in
8 - output coupling stub
9 - input coupling stub
10 - cathode capacitive stub
11 - air-cooling tube

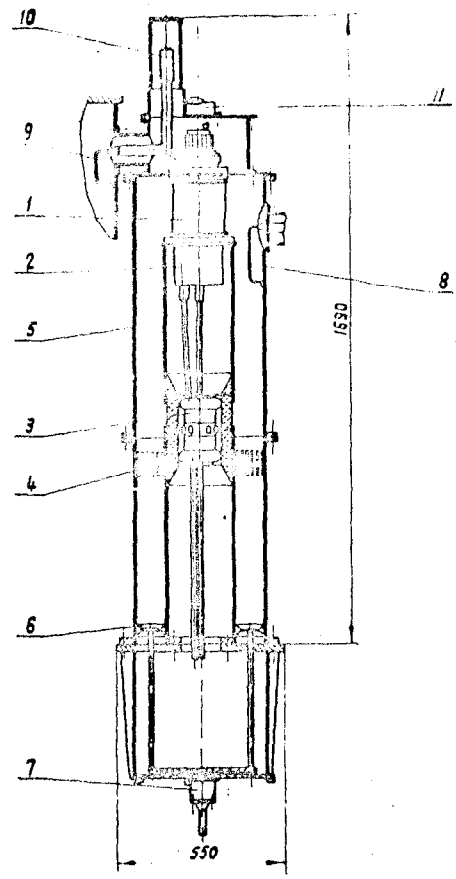

Рис. 4. Генератор на ГИ-24А.
1- лампа ГИ-24а; 2 - бачок водяного охлаждения лампы; 3 - анодная разделительная емкость; 4 - изолятор; 5 - анодная линия; 6 - плунжер; 7 - электрический привод; 8 - выходная петля связи; 9 - входная петля связи; 10 - катодный емкостной шлейф; 11 - труба воздушного охлаждения.

F i g u r e 5 :

The preamplifier

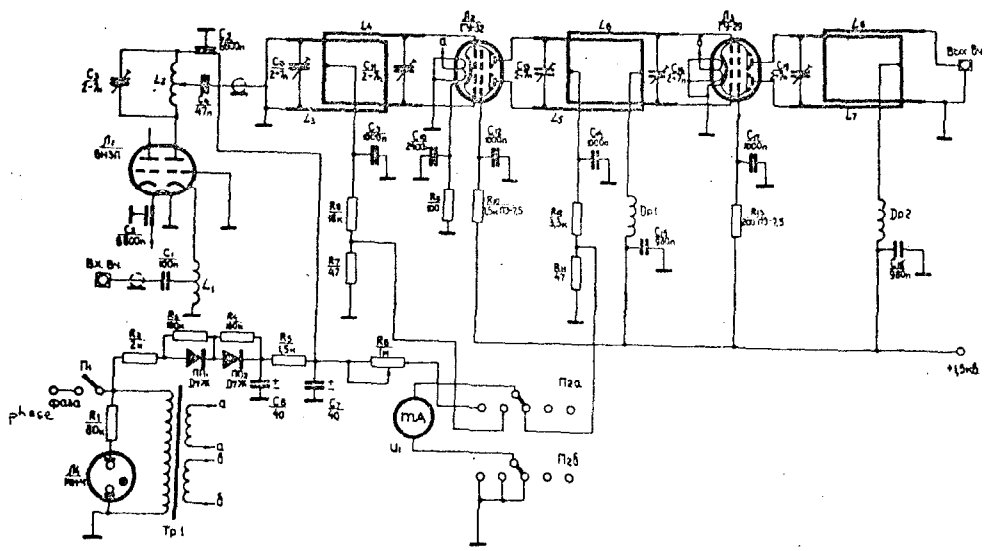

Рис. 5. Электрическая схема предварительного усилителя.

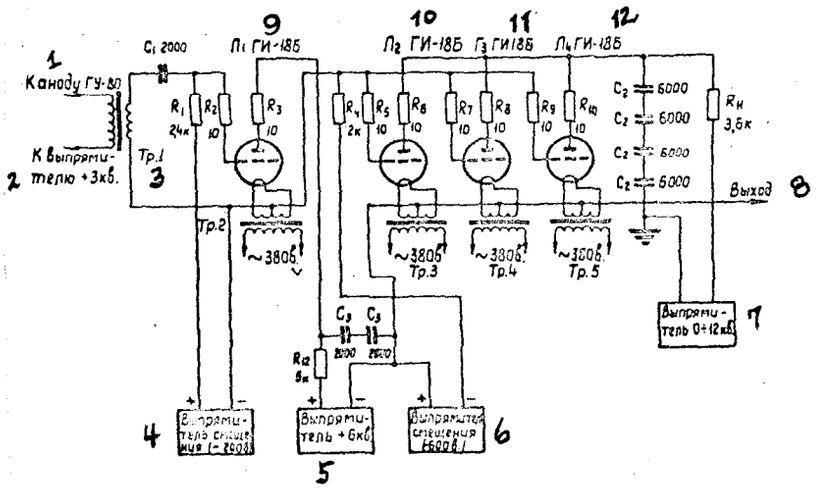

Рис. 6. Принципиальная схема оконечных каскадов импульсного модулятора.

Figure 6: Basic circuit of the final stages of the pulse modulator

Key:
1 - To anode GU-80
2 - To rectifier + 3kv
3 - Tr.1, etc.
4 - Bias rectifier (-200 v)
5 - Rectifier + 6 kv
6 - Bias rectifier (- 600 v)
7 - Rectifier 0 - 12 kv
8 - Output
9 - L_1 GI-185
10 - L_2 GI-185
11 - G_3 GI-185
12 - L_4 GI-185

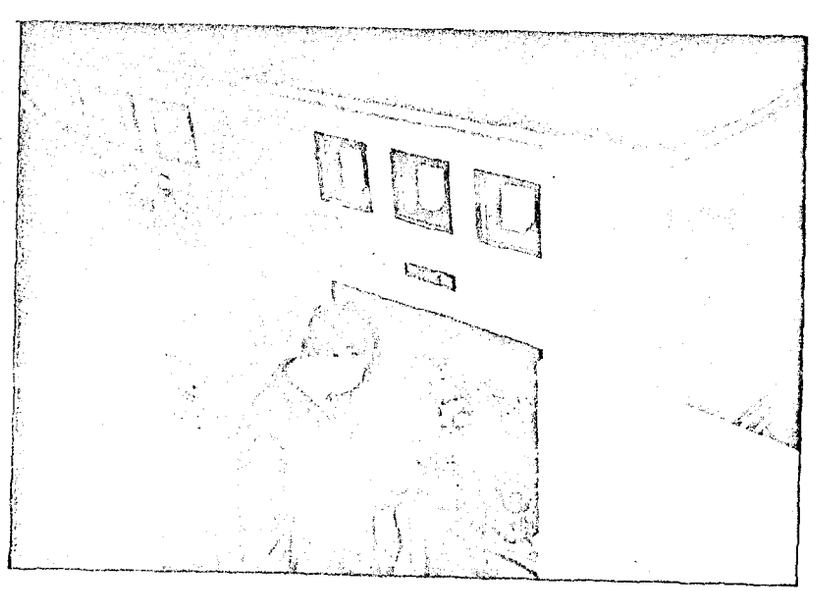

Figure 7: Photograph of the pulse modulator

Рис. 7. Внешний вид импульсного модулятора.

Figure 8:

Control desk

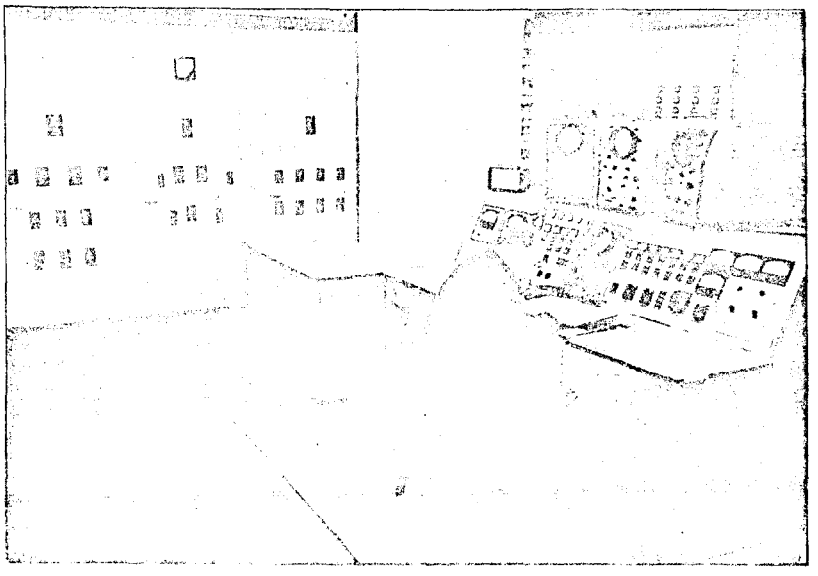

Рис. 8. Пульт управления.

Figure 9:

Experimental proton-capture factor as a function of the accelerating proton synchrotron frequency $f_{1(t)}$ at the instant of capture (beam energy 10 GeV, energy spread $\pm$ 1.7 Mev)

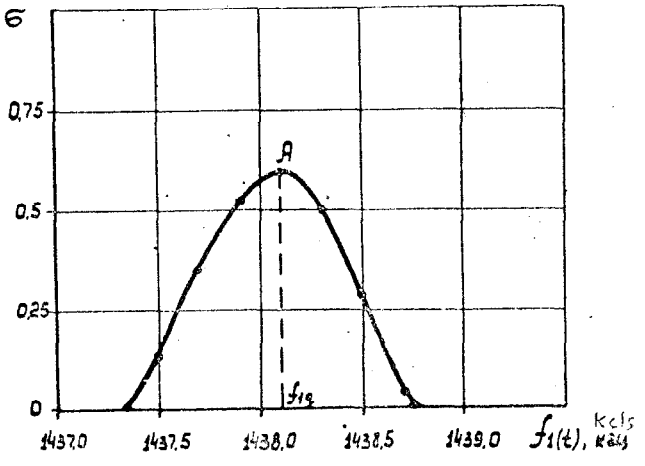

Рис. 9. Экспериментальная зависимость коэффициента перезахвата протонов в режим кратного ускорения σ от ускоряющей частоты синхрофазотрона в момент перезахвата $f_1(t)$ (E =10Гэв, $\Delta E = \pm 1{,}7$ Мэв).

□□□□□□□□□□□□□□□□□□□□□□□□□□□□□□□□□□□□

Translation supplied by

addis TRANSLATORS INTERNATIONAL
129 Pope Street
Menlo Park, Calif. 94025 U.S.A.
Tel. (415) 322-6733
Cable: addistran menlopark

JAN 1966
RECEIVED
Library
SLAC